

Properties of electron swarm parameters in Tetrahydrofuran

Dr.Mohammad M. Othman

Department of Physics, College of Education, University of Salahaddin-Hawler, KRG, Iraq.
Email id: muhamad.othman@su.edu.krd

Abstract

Reported electron collision cross sections data in the energy range ~ 0 to 300 eV (see section 3) from gaseous biomolecule Tetrahydrofuran (THF) have been used to calculate the electron energy distribution function and electron (EEDF) and swarm parameters for electrically excited THF, using a two-term solution of the Boltzmann equation. The electron swarm parameters namely (mean energy, drift velocity, diffusion coefficient, electron mobility, characteristic energy, attachment and ionization coefficient), at room temperature and atmospheric pressure are presented over a wide range of applied electric field strength E/N (E is the electric field and N is the gas number density) varying from 0.1 to 1000 Td ($1\text{Td}=10^{-17}\text{ Vcm}^2$). The EEDF found to be non-Maxwellian. The electron swarm parameters are compared with those calculated using multi term kinetic theory and experimentally using the pulsed Townsend technique. The influence of inelastic cross section on the calculated transport parameters is also explained.

Keywords: THF, swarm parameters, cross sections, Kinetics, electron Boltzmann equation.

1. Introduction

Low temperature plasma, ionized gas and liquid represented a state of matter of neutral atoms and molecules, radicals, excited state, ions and electrons with energies with small ionization degree and electron energies up to 10 eV. At low pressure the energies of electron and ion fluxes ranging from few to 100 eV are used in many industrial application such as plasma enhanced chemical vapor deposition (PECVD) is widely used to modulate the surface by etching deposition and fabricate thin films, low dielectric constant films, plasma agriculture and innovative food cycles, plasma catalysis, flow control material processing, synthesis and plasma photonic crystals [2], gaseous electronics [44] and in plasma medical application such as electro surgery (Stalder et al., 2006), tissue engineering [8], surface modification of biocompatible [46], and the sterilization of heat-sensitive materials and instruments [35]. While many industrial application of plasma are operate close to thermal equilibrium [6,30,59-67] such that coupled plasma discharges, arc, and microwave. Also the interaction of non-equilibrium plasma with gas phase and liquid state important in health care and material science [9]. In radiation and medicine (10-14), high-energy ionizing radiation e.g., α -particles, protons, heavy ions, γ -rays, and X-rays, use in radiotherapy and radiodiagnostic exams, when incident the biomolecular model systems or living cells leads to loss genetic information, cell death and genetic mutation [29] by secondary electrons when the energy of low-energy electrons (LEEs) below 20 eV, it can induce damage to DNA.[36] show that the low-energy electrons (LEEs) induce damage in DNA, as well as to basic DNA components such as bases[1], deoxyribose sugar [45,68-74] and the phosphate group [24,43] via the formation of negative ions or resonances, these processes occurs via dissociative electron attachment (DNA).

The interaction of positron with human tissue and biological matter is important key for the medical field, in fact as the electron and positrons are thermalize in biological matter and human

tissue, the annihilation γ -rays emitted by annihilation of two particles such technique used in imaging application called positron emission tomography (PET) [14]. Furthermore, the interaction of electrons with water play important role in study of the behavior of biomolecules, water vapour used as a replacement for the bimolecular in process of radiolysis tracks [40]. Tetrahydrofuran molecule (THF, C_4H_8O), or oxolane, is the best matter in gas phase used to study the biomolecules matter after water[48], can be viewed as a sugar-like component of the backbone of DNA. The backbone of DNA consists as a series of Tetrahydrofuran (THF) molecules held together by phosphate bonds, also Tetrahydrofuran (THF) is an important component of RNA [51,75-83]. More recently, Tetrahydrofuran has been investigated experimentally and theoretically to understanding the low energy electron collisions and the dynamic of energy deposition in DNA [52,53,54], For plasma interaction with biological matter, the electron collision cross sections play the important role to study the electron transport parameters in gaseous systems. Several electron collision cross sections have been measured experimentally and derived theoretically for Tetrahydrofuran. These includes, quasielastic (momentum transfer and rotational) [15,17,4,31,7,28,16,58,84-89], electronic excitation [58] vibrational excitation [4,17,18], ionization

Dissociative electron attachment cross sections [3,34,48], in addition to differential elastic and total scattering cross sections [56,39,51,7,11,90]. Chronologically, six full sets of Tetrahydrofuran (THF) cross sections (momentum transfer, vibrational excitation, electronic excitation ionization and attachment cross sections) have been proposed experimentally and theoretically over various electron energy ranges: by [27] for electron incident energies between 0.1 eV to 300 eV, [26] for electron incident energies from 1 eV to 10KeV, [12] for energies ranging from 30 eV to 1000 eV, [50] for electron energies between the ionization threshold to 5000 eV, and [12] modified the [27] cross-section sets by the first measurement of electron swarm parameters in pure gaseous Tetrahydrofuran (THF), using inverse swarm method. Thereafter, who refined the [12] cross-section sets by performing and analyzing the swarm parameters fo THF-Ar and THF-N₂ mixtures.

The swarm parameters has a long history from the early studies to more recent investigation [47, 22]. Theoretically swarm parameters may be calculated using Monte Carlo Simulation or Boltzmann equation analysis using electron energy distribution function (EEDF) with the available sets of cross sections. The EEDF calculated by the electron energy gain and loss due to acceleration with electric field and electrons collision [33].

The electron swarm parameters of THF, namely, drift velocity, electron mean energy, ionization and attachment coefficients, are widely studied in the literature [27,12]. These swarm parameters are also calculated in THF-H₂O [52] and THF-Ar and THF-N₂ [55] gas mixtures. More recently, the binary mixtures of THF-Ar are studied by [48,91].

In the present work we have calculated the electron swarm parameters of Tetrahydrofuran (THF) based on the two term solution of Boltzmann transport equation that is solved for values of E/N ranging from 0.1 to 1000 Td (1Td= 10^{-17} V.cm²) using the NOMAD code.

2.The Boltzmann equation

The general formulation of Boltzmann equation is

$$\frac{\partial f}{\partial t} + \mathbf{V} \cdot \nabla_r f - \frac{eE}{m} \cdot \nabla_v f = \left(\frac{\partial f}{\partial t} \right)_c \quad (1)$$

Where $f(r, v, t)$ is the velocity distribution function at time t and special location r , here v is the electron velocity in the field direction. So that $f(r, v, t)$ is a function of velocity only, when the electric field is independent of space and time, then $f(r, v, t) \rightarrow f(v, t)$, $\nabla_r f = 0$, and equation (1) becomes,

$$\frac{\partial f}{\partial t} + -\frac{eE}{m} \cdot \nabla_v f = \left(\frac{\partial f}{\partial t} \right)_c \quad (2)$$

Where $\left(\frac{\partial f}{\partial t} \right)_c$ is the collision integral, which depends on electron collision processes, e is electron charge, m is the electron mass and E is the dc applied electric field. The convenient procedure for description the motion in uniform dc electric field is to explain the electron distribution function $f(r, v, t)$ in terms of series of spherical harmonic Legendre function of the form [5],

$$f(r, v, t) = f_o(v) + P_1(\cos\theta)f_1(v) + P_2(\cos\theta)f_2(v) + \dots \quad (3)$$

If the momentum transfer cross section is large compared with the collisional energy rate, a two-term expansion of the velocity distribution will be sufficient.

$$f(v) = f_o(v) + \frac{\bar{v}}{v} f_1(v) \quad (4)$$

Where $f_o(v)$ and $f_1(v)$ represent the isotropic and anisotropic parts are function of magnitude of v only, and $f_o(v) \gg f_1(v)$. The expansion of equation (4) is to be substituted into equation (3), and converting velocity to a function of energy ($u = mv^2/2$), and where the electron energy distribution function $f(u)$ obeys to the normalization condition,

$$\int_0^\infty f(u) \sqrt{u} du = 1 \quad (5)$$

the steady state electron energy distribution function $f(u)$ obtained by solution of the Boltzmann equation with the superelastic term and without the superelastic term, may be written in the form,

$$\begin{aligned} & \frac{E^2}{3} \frac{d}{du} \left(\frac{u}{NQ_m^e(u)} \frac{df_o(u)}{du} \right) + \frac{2m}{M} \frac{d}{du} (u^2 NQ_m^e(u) f_o(u)) \\ & + \frac{2mK_B T_g}{Me} \left(u^2 NQ_m^e(u) \frac{df_o(u)}{du} \right) \\ & + \sum_j [(u + u_j) f_o(u + u_j) N_o Q_j(u + u_j) - u f_o(u) N_o Q_j(u)] \\ & + \sum_j [(u - u_j) f_o(u - u_j) N_j Q_{-j}(u - u_j) - u f_o(u) NQ_{-j}(u)] = 0 \end{aligned} \quad (6)$$

The superelastic cross-section Q_{-j} can be written as,

$$Q_{-j} = \frac{u + u_j}{u} Q_j(u + u_j) \quad (6)$$

Here,

$$Q_m^e(u) = Q_m(u) + \sum_j Q_j(u) + Q_i(u) + Q_a(u) \quad (7)$$

Where $Q_m^e(u)$ denotes an effective collision frequency for momentum transfer, M , K_B , u , N are the molecular mass, Boltzmann constant, electron energy and the gas density respectively, $Q_m(u)$ is the momentum transfer cross-sections related to the total cross section $Q_m(u) = Q_T(u)(1 - \cos\theta)$, where θ is scattering angle. $Q_i(u)$, $Q_e(u)$, $Q_a(u)$ and u_J are the electron cross sections for excitation (rotational, vibrational, electronic), ionization, attachment and energy loss due to collisional excitation respectively. The last two term is the influence of superelastic collision it occurs at low electric field, $Q_{-J}(u)$ is superelastic cross-section, u_J energy gain due to superelastic collision.

The initial electron energy distribution function EEDF with a mean electron energy $\bar{u} = 1.5K_B T_e$ was chosen as Maxwellian with temperature T_e , normalized by equation (5),

$$f(u) = \left(\frac{2}{\sqrt{\pi}} \right) (K_B T_e)^{-\frac{3}{2}} \exp\left(\frac{-u}{K_B T_e} \right) \quad (8)$$

Using the electron energy distribution function one can calculate the electron swarm parameters as follows [42,29]

The mean electron energy,

$$\bar{u} = \int_0^{\infty} u^2 f_o(u) du \quad (9)$$

The density-normalized electron mobility μ_e

$$\mu_e N = -\frac{1}{3} \left(\frac{2e}{m} \right)^{\frac{1}{2}} \int_0^{\infty} \frac{u}{Q_m^e(u)} \frac{df_o(u)}{du} du \quad (10)$$

The electrons drift velocity,

$$v_d = -\frac{1}{3} \sqrt{\frac{2e}{m}} \frac{E}{N} \int_0^{\infty} \frac{u}{Q_m^e(u)} \frac{\partial f_o(u)}{\partial u} du \quad (11)$$

The density-normalized transverse diffusion coefficient,

$$D_T N = \frac{1}{3} \left(\frac{2e}{m} \right)^{\frac{1}{2}} \int_0^{\infty} \frac{u f_o(u)}{Q_m^e(u)} du \quad (12)$$

The characteristic energy u_k ,

$$u_k = \frac{D_T e}{\mu_e} \quad (13)$$

The reduced-density ionization coefficient α/N is given by [41]

$$\frac{\alpha}{N} = \frac{1}{v_d} \left(\frac{2e}{m} \right)^{\frac{1}{2}} \int_i^{\infty} Q_i(u) u f_o(u) du \quad (14)$$

where $Q_i(u)$ is the ionization cross-section.

The reduced-density attachment coefficient η/N is given by:

$$\frac{\eta}{N} = \frac{1}{v_d} \left(\frac{2e}{m} \right)^{1/2} \int_a^\infty Q_a(u) f_o(u) du \quad (15)$$

where $Q_a(u)$ is the attachment cross-section.

Electron swarm parameters were calculate using collision cross section for a THF vapour number density $N=7.3765 \times 10^{21} \text{ cm}^{-3}$, which is equivalent to 1 atm at 298 K.

1. Cross Section

The electron energy distribution function (EEDF) and electron swarm parameters in gaseous Tetrahydrofuran (THF, $\text{C}_4\text{H}_8\text{O}$) calculated from the sets cross section (elastic and inelastic), this sets includes 21 collision processes: one momentum transfer cross section (Q_m) taken from (Garland, et al., 2013; Casy, et al., 2017, 12 vibration excitation (Q_{v1} , Q_{v2} , Q_{v3} , Q_{v4} , Q_{v5} , Q_{v6} , Q_{v7} , Q_{v8} , Q_{v9} , Q_{v10} , Q_{v11} , Q_{v12}) with threshold energy 0.228, 0.72 0.114, 0.134, 0.18, 0.363, 0.45, 0.65, 0.15, 0.083, 0.27 and 0.330 eV respectively are taken from and six electronic excitation cross sections of have been used based on the energy loss spectra of [23]. The attachment cross sections of have been used, these lie between the values of and the values of [21] with threshold energy of 0.28 eV, lying between the threshold energy of 1 eV for [27] and 0.08 eV [21]. The ionization cross sections with threshold energy 0.955 eV of have been used, and these are in good agreement with [25] and [19].

4. Results and Discussion

To solve the electron energy distribution function (EEDF) based on the two-term solution of Boltzmann equation, the data of electron collision cross-sections of THF is explained in previous section, used as main input data to calculated electron swarm parameters.

The electron energy distribution function EEDF as function of electron energy, are obtained by using two-term approximation solution of Boltzmann equation method (Eq. 6), at different values of electric field strength E/N (E : electric field, N : gas number density). Electric field strength E/N , expressed in unit of Townsend ($1\text{Td}=10^{-17} \text{ V.cm}^2$).

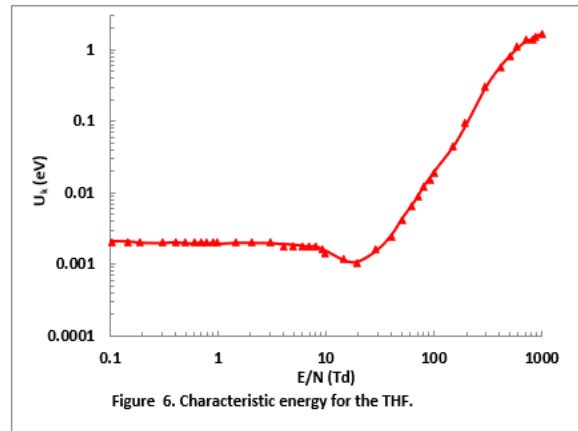
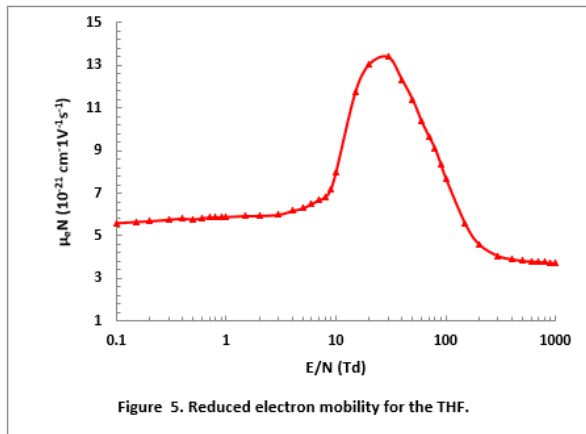
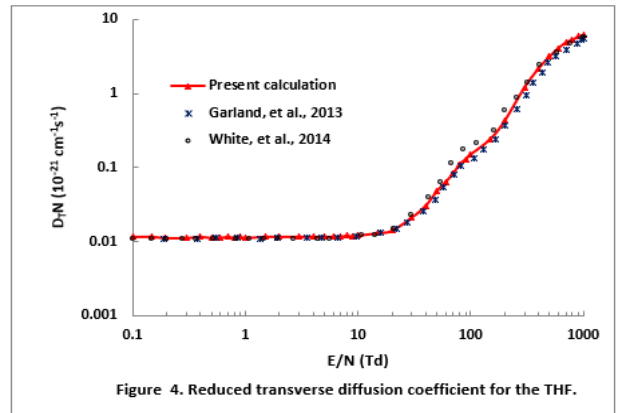
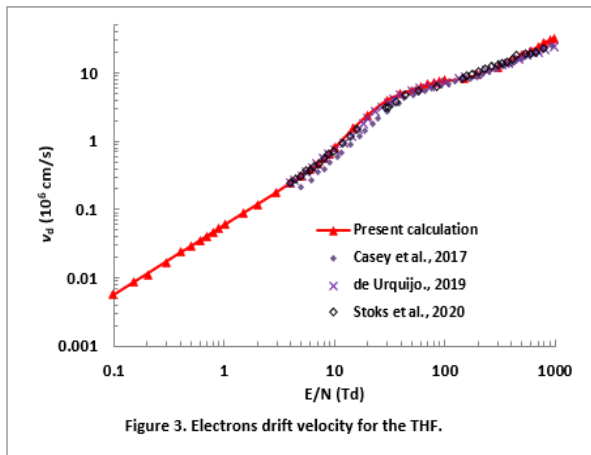
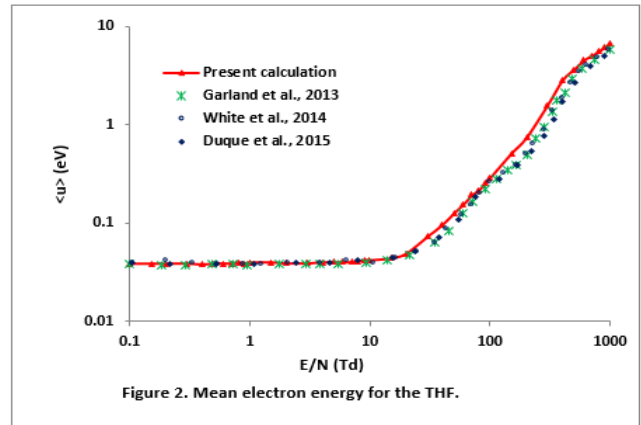
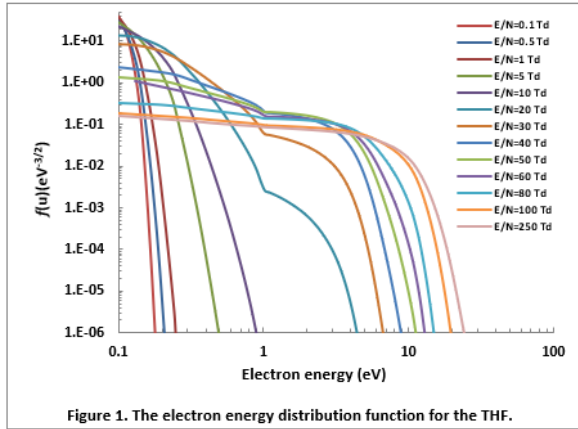
The calculated electron energy distribution function EEDF for a dc field in THF at different values of E/N at temperature 298 K and pressure 1 atm are shown in figure 1. It is found that at lowest electric field strength E/N , the electron energies are thermal and the electron energy distribution function EEDF is Maxwellian (Eq. 8) with mean electron energy $\bar{u} = 1.5 K_B T_e$, the Maxwellian distribution function normalized by Eq. 5, where T_e is electron temperature in unit of eV.. At $E/N < 20 \text{ Td}$, EEDF drops sharply at after several (eV) the Maxwellian function's will appear as straight lines, because the elastic cross-section is constant at low electric field and the vibrational cross section increases around 0.1 eV and decrease when electron energy greater than 1 eV. Therefore, in this region the degree of ionization is very small and the energy created from electric field is mainly used for vibrational excitation at $E/N < 20 \text{ Td}$. However, as the E/N is increased the EEDF located at higher energy range, the EEDF is clearly non-Maxwellian, and has a shoulder at about 2 eV when $E/N \geq 20 \text{ Td}$, due to the large electronic excitation and vibrational cross-section. As shown in figure 1, the tail of the distribution function shift to higher energy due to inelastic collision which reflects the dominant electron-molecule energy exchange processes in this region more ionization or excitation collision occurs.

Figures 2-8, we present results for electron swarm parameters in THF, including mean energy, drift velocity, diffusion coefficient, mobility, ionization and attachment coefficient. The results presented are calculated and analyzed using two-term solution of the Boltzmann equation by a balance between power input from an applied electric field E and energy loss rate via electron collisions. All results are calculated as a function of the reduced electric field E/N over a wide range varying from 0.1 to 1000 Td, ($1\text{Td}=10^{-17}\text{ Vcm}^2$) at fixed temperature 298 K and pressure 1 atm. Figure 2 demonstrated mean electron energy as a function of E/N , in the low electric field strength $E/N < 10$ Td the mean energy is in thermal equilibrium, it is essentially isotropic remain nearly constant, as we move to higher field the mean energy rapidly increases with increasing E/N , this is because at high energy region the inelastic processes are dominated. The behavior of the mean electron energy is also reflected in the electron drift velocity and diffusion coefficient. It is seen the present calculation agree well with the theoretical values of [53, 23].

The present values of drift velocity for THF are shown in figure 3, along with the previous experimental values of [12] and theoretical values are displayed in the same figure. A good agreement has been shown over the entire range of E/N . It is evident that the experimental data of fall below present results, the difference is up to about 15% over the range of $E/N < 40$ Td. As shown in figure 3, the calculated drift velocity in thermal equilibrium with background THF vapour from 0.1 to 10 Td linearly increase, where elastic and vibrational collision are dominate. Around 20 to 40 Td a plateau in the drift velocity is observed due to the effect of the electronic excitation. At high reduce electric field strength $E/N > 100$ Td the ionization channel is dominate, the drift velocity increase up to the highest calculated value at 1000 Td.

The reduced transverse diffusion coefficient $D_T N$ for pure THF vapour is shown in figure 4. The present calculation was found in good agreement with theoretical values of [53]. The normalized reduced electron mobility $\mu_e N$ is shown in figure 5, at low E/N values the electron mobility is in thermal equilibrium, when E/N is around 30 Td, a maximum values can be observed, then the electron mobility start to decrease with increasing E/N , because at $E/N > 30$ Td the attachment coefficient decrease the number of electrons. The behavior of characteristic energy eD_T/μ_e displays in figure 6.

Figure 7, is illustrated the reduced-density attachment coefficient η/N in THF as a function of E/N , in comparison with the experimental values of and as well as the theoretical values. Throughout the range of $5 \leq E/N \leq 100$ Td, good agreements has been observed. At low reduced electric field, $E/N < 20$ Td the electronegative region observed, in this region the reduced attachment coefficient decreasing with increasing E/N until approximately 30 Td, the resonance region appear at around 40 Td, then start to increase up to 70 Td, again start to decrease, around 100 Td the ionization channel dominated. This is because around 20.5 eV a large increase in the magnitude of the dissociation electron attachment DEA observed approximately equal to $0.0033 \times 10^{-16}\text{ cm}^2$. The reduced-density ionization coefficient α/N in THF is shown in figure 8. The present values are compared with the theoretical values of and with the measured values. Throughout the range of $100 \leq E/N \leq 1000$ Td, the theoretical results of and experimental results slightly lower compare with the present results. The coherent results obtained confirmed that two-term solution of Boltzmann equation analysis of the present study is valid.



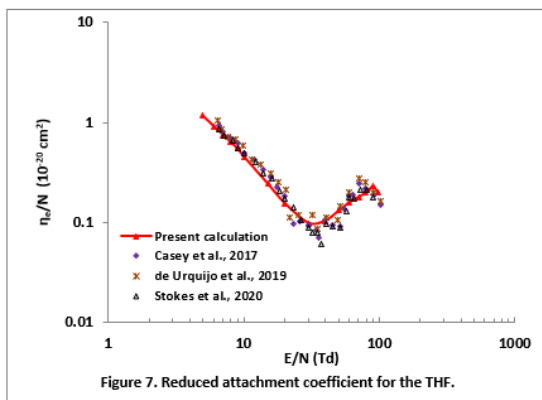


Figure 7. Reduced attachment coefficient for the THF.

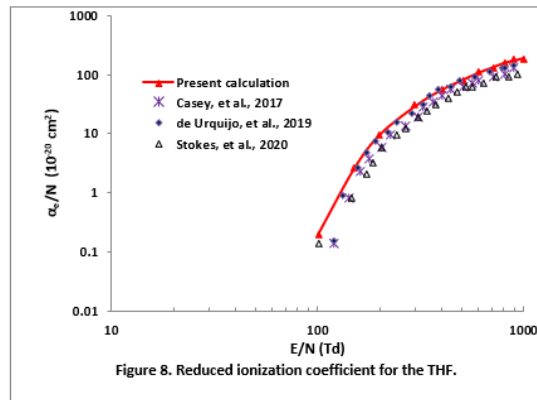


Figure 8. Reduced ionization coefficient for the THF.

5. Conclusion

The Boltzmann equation analysis and the set of cross sections important in the area of low-temperature plasma physics. In the present work, we have examined the behavior of electrons in applied uniform dc electric fields as a function of reduced electric field strength E/N . The two-term solution results give values for EEDF and mean energy, drift velocity, transverse diffusion coefficient, electron mobility, characteristic energy, attachment and ionization coefficient as a function of E/N in the range between 0.1 to 1000 Td. These results were obtained based on binary collisions of electrons with THF molecule. A good agreement between the calculated and previous theoretical and experimental values is observed.

References

1. Abdoul-Carime, H., Gohlke, S., and Illenberger, E., (2004). Site-specific diiodination of DNA bases by slow electrons at early stages of irradiation, *Phys. Rev. Lett.*, 92(16), 168103 (4pp).
2. Adamovich, I; Baalrud, S D; Bogaerts, A; Bruggeman, P J; Cappelli, M; Colombo, V; Czarnetzki, U; Ebert, U; Eden, J G; Favia, P; Graves, D B; Hamaguchi, S; Hieftje, G; Hori, M; Kaganovich, I D; Kortshagen, U; Kushner, M J; Mason, N J; Mazouffre, S; Thagard, S Mededovic; Metelmann, H-R; Mizuno, A; Moreau, E; Murphy, A B; Niemira, B A; Oehrlein, G S; Petrovic, Z Lj; Pitchford, L C; Pu, Y-K; Rauf, S; Sakai, O; Samukawa, S; Starikovskaia, S; Tennyson, J; Terashima, K; Turner, M M; van de Sanden, M C M; Vardelle, A. (2017). The 2017 Plasma Roadmap: Low temperature plasma science and technology, *J.Phys. D: Appl. Phys.*, 50(32), 323001 (46pp).
3. Aflatooni, K., Scheer, A., Mand Burrow, P. D. (2006). Total dissociative electron attachment cross sections for molecular constituents of DNA, *J. Chem. Phys.*, 125(5), 054301 (5pp).
4. Allan, M. (2007). Absolute angle-differential elastic and vibrational excitation cross sections for electron collisions with tetrahydrofuran, *J. Phys. B: At. Mol. Opt. Phys.*, 40(17), 3531–3544.
5. Allis, W. P. (1956). Motions of ions and electrons, *Handbuch der Physik*, vol. 21 (Springer, Berlin).

7. Armelle, V., Chriatian, M., (.....), and Petri, V. **(2016)**. The 2016 thermal spray roadmap, *J. of Thermal Spray*, 25(8), 1376-1440.
8. Baek, W. Y., Bug, M., Rabus, H., Gargioni, E., and Grosswendt, B. **(2012)**. Differential elastic and total electron scattering cross sections of tetrahydrofuran, *Phys. Rev. A* 86(3), 032702 (15pp).
9. Blakely, E. A., Bjornstad, K. A., Galvin, J. E., Monteiro, O. R., and Brown, I. G. **(2002)**. Selective neuron growth on ion implanted plasma deposited surface, in *proc. IEEE Intr. Conf. Plasma Sci.*, pp. 253.
10. Bruggeman, P J; Kushner, M J; Locke, B R; Gardeniers, J G E; Graham, W G; Graves, D B; Hofman-Caris, R C H M; Maric, D; Reid, J P; Ceriani, E; Fernandez Rivas, D; Foster, J E; Garrick, S C; Gorbanev, Y; Hamaguchi, S; Iza, F; Jablonowski, H; Klimova, E; Kolb, J; Krcma, F; Lukes, P; Machala, Z; Marinov, I; Mariotti, D; Mededovic Thagard, S; Minakata, D; Neyts, E C; Pawlat, J; Petrovic, Z Lj; Pflieger, R; Reuter, S; Schram, D C; Schröter, S; Shiraiwa, M; Tarabová, B; Tsai, P A; Verlet, J R R; von Woedtke, T; Wilson, K R; Yasui, K; Zvereva, G. (2010). Plasma-liquid interactions a review and roadmap, *Plasma Sources Sci. Technol.*, 25, 053002 (59pp.).
11. Builth-Williams, J. D., et al. **(2013)**. A dynamical (e,2e) investigation of the structurally related cyclic ethers tetrahydrofuran, tetrahydropyran, and 1,4-dioxane, *J. Chem. Phys.*, 139(13), 034306 (8pp).
12. Bug, M.U., Yong Baek, W., Rabus, H., Villagrasa, C., Meylan, S., and Rosenfeld, A. B. **(2017)**. An electron-impact cross section data set (10 eV – 1 keV) of DNA constituents based on consistent experimental data: a requisite for Monte Carlo simulations, *Radiat. Phys. Chem.*, 130, pp. 459–479.
13. Casey, M. J. E., de Urquijo, J., Serkovic Loli, L. N., Cocks, D. G., Boyle, G. J., Jones, D. B., Brunger, M. J., and White, R. D. (2017) . Self-consistency of electron-THF cross sections using electron swarm techniques, *J.Chem. Phys.*, 147(19), 195103 (16pp).
14. Champion, C. **(2013)**. Quantum-mechanical predictions of electron-induced ionization cross sections of DNA components, *J. Chem. Phys.*, 138(18), 184306 (8pp).
15. Cherry, S. R., Sorosen, J. A., and Phelps, M. E. **(2003)**, *Physics in nuclear medicine*, Sounders, Philaddphia.
16. Colyer, C. J., Vizcaino, V., Sullivan, J. P., Brunger, M. J., and Buckman, S. J. (2007). Absolute elastic cross-sections for low-energy electron scattering from tetrahydrofuran, *New J. Phys.*, 9(2), 41 (11pp).
17. Chiari, Luca, Anderson, Emma, Tattersall, Wade, Machacek, J. R., Palihawadana, Prasanga, Makochekanwa, Casten, Sullivan, James P., García, Gustavo, Blanco, Francisco, McEachran, R. P., Brunger, M. J., Buckman, Stephen J. **(2013)**. Total, elastic, and inelastic cross sections for positron and electron collisions with tetrahydrofuran, *The Journal of Chemical Physics*, 138(7), 074301 (15pp).
18. Dampe, M., Milosavljević, A. R., Linert, I., Marinković, B. P., and Zubek, M. **(2007)**. Differential cross sections for low-energy elastic electron scattering from tetrahydrofuran in the angular range 20°–180°, *Phys. Rev. A*, 75(4), 042710 (7pp).
19. Dampe, M., Linert, I., Milosavljević, A. R. and Zubek, M. **(2007a)**. Vibrational excitation of tetrahydrofuran by electron impact in the low energy range, *Chem. Phys. Lett.*, 443(1-3), 17–21.

20. Dampc, M., Szymańska, E., Mielewska, B. and Zubek, M. **(2011)**. Ionization and ionic fragmentation of tetrahydrofuran molecules by electron collisions, *J. Phys. B: At. Mol. Opt. Phys.*, 44(5) 055206 (7pp).
21. Deng, Y., and Xiao, D. **(2014)**. Analysis of the insulation characteristics of CF₃I gas mixtures with Ar, Xe, He, N₂, and CO₂ using Boltzmann equation method, *Japanese Journal of Applied Physics*, 53(9), 096201 (7pp).
22. de Urquijo, J., Casey, M. J. E., Serkovic-Loli, L. N., Cocks, D. G., Boyle, G. J., Jones, D. B., Brunger, M. J. and White, R. D. **(2019)**. *J. Chem. Phys.*, 151(5), 054309 (17pp).
23. Do, T. P. T., Leung, M., Fuss, M., Garcia, G., Blanco, F., Ratnavelu, K., and Brunger, M. J. **(2011)**. Excitation of electronic states in tetrahydrofuran by electron impact, *J. Chem. Phys.*, 134(14), 144302 (8pp).
24. Duque, H. V., Do, T. P. T., Lopes, M. C. A., Konovalov, D. A., White, R. D., Brunger, M. J. and Jones, D. B. **(2015)**. The role of electron-impact vibrational excitation in electron transport through gaseous tetrahydrofuran, *J. Chem. Phys.*, 142, 124307 (7pp).
25. Elahe Alizadeh, Thomas, M. Orlando, and Leon Sanche, **(2015)**. Biomolecular damage induced by ionizing radiation: The direct and indirect effects of low-energy electrons on DNA, *Annu. Rev. Phys. Chem.*, 66(1), 379-398.
26. Fuss, M., Muñoz, A., Oller, J. C., Blanco, F., Almeida, D., Limão-Vieira, P., Do, T. P. D., Brunger, M. J. and García, G. **(2009)**. Electron-scattering cross sections for collisions with tetrahydrofuran from 50 to 5000 eV, *Phys. Rev. A* 80(5), 052709 (6pp).
27. Fuss, M. C., Sanz, A. G., Blanco, F., Limão-Vieira, P., Brunger, M. J., and García, G. **(2014)**. Differential and integral electron scattering cross sections from tetrahydrofuran (THF) over a wide energy range: 1–10 000 eV *Eur. Phys. J. D*, 68(6), 161 (6pp).
28. Garland, N. A., Brunger, M. J., Garcia, G., de Urquijo, J., and White, R. D. **(2013)**. Transport properties of electron swarms in tetrahydrofuran under the influence of an applied electric field, *Phys. Rev. A*, 88(6), 062712 (10pp).
29. Gauf, A., Hargreaves, L. R., Jo, A., Tanner, J., Khakoo, M. A., Walls, T., Winstead, C., and McKoy, V. **(2012)**. Low-energy electron scattering by tetrahydrofuran, *Phys. Rev. A* 85(5), 052717 (8pp).
30. Hangelaar, G. J. M. and Pichford, L. C. **(2005)**. Solving the Boltzmann equation to obtain electron transport coefficients and rate coefficients for fluid models. *Plasma Sources Sci. Technol.*, 14(4), pp. 722-733.
31. Hall, E. J., and Giaccia, A. J. **(2018)**. *Radiobiology for the Radiologist*, 8ed, Philadelphia: Lippincott Williams and Wilkins.
32. Hebrlein, J., and Murpby, A. B. **(2008)**. Thermal plasma waste treatment, *J. Phys. D: Appl. Phys.*, 41(5), 053001 (20pp).
33. Homem, M. G. P., Sugohara, R. T., Sanches, I. P., Lee, M. T., and Iga, I. **(2009)**. Cross sections for elastic electron collisions with tetrahydrofuran, *Phys. Rev. A*, 80(3), 032705 (7pp).
34. Itikawa, Y. **(2007)**. *Molecular processes in plasma*, Tokyo, Japan.
35. Janečková, R., May, O., Milosavljević, A. and Fedor, J. **(2014)**. Partial cross sections for dissociative electron attachment to tetrahydrofuran reveal a dynamics-driven rich fragmentation pattern *Int. J. Mass Spectrom.* 365-366, pp. 163–168.

36. Khakoo, M. A., Orton, D., Hargreaves, L. R., and Meyer, N. **(2013)**. Electron-impact vibrational excitation of tetrahydrofuran, *Phys. Rev. A* 88(1), 012705 (6pp).
37. Laroussi, M. **(2003)**. Plasma-based sterilization, in *Proc. Intr. Conf. Phenomena Ionized Gases*, Greifswald, Germany, pp. 11-12.
38. Martin, Frédéric; Burrow, Paul D.; Cai, Zhongli; Cloutier, Pierre; Hunting, Darel; Sanche, Léon, **(2004)**. DNA strand breaks induced by 0-4 eV electrons: The role of shape resonances, *Phys. Rev. Lett.*, 93(6), 068101 (4pp).
39. Mo'zejko, P., Ptasińska-Denga, E., Domaracka, A., and Szmytkowski, C., **(2006)**. Absolute total cross-section measurements for electron collisions with tetrahydrofuran, *Phys. Rev. A*, 74(1), 012708 (5pp).
40. Mo'zejko, P., and Sanche, L. **(2005)**. Cross sections for electron scattering from selected components of DNA and RNA, *Radiat. Phys. Chem.* 73(2), 77–84.
41. Muñoz, A., Blanco, F., Garcia, G., Thorn, P. A., Brunger, M. J., Sullivan, J. P., and Buckman, S. J. **(2008)**. Single electron tracks in water vapour for energies below 100 eV, *International Journal of Mass Spectrometry*, 277(1-3), pp. 175-179.
42. Othman, M. M., Salih, I. H. and Taha, S. A. **(2020)**. Electron transport properties in tetramethylsilane vapour, *Solid State Technology*, 63(6), pp. 10188-10200.
43. Othman, M. M., Taha, S. A., and Sailh, I. H. **(2019)**. Solving of the Boltzmann transport equation using two-term approximation for pure electronegative gases (SF₆, CCl₂F₂). *ZANCO Journal of Pure and Applied Sciences*, 31(s4), pp. 7-25.
44. Pan, X., and Sanche, L. **(2005)**. Mechanism and site of attack for direct damage to DNA by low energy electron, *Phys. Rev. Lett.*, 94(19), 198104 (4pp).
45. Petrović, Z. Lj., Dujko, S., Marić, D., Malović, G., Nikitović, A., Šašić, O., Jovanović, J., Stojanović, V., and Radmilović-Radenović, M. **(2009)**. Measurement and interpretation of swarm parameters and their application in plasma modeling, *J. Phys. D: Appl. Phys.*, 42(19), 194002 (33pp).
46. Ptasińska, S., Denifls, S., Scheier, P., and Mark, T. D. **(2004)**. Inelastic electron interaction (attachment/ionization) with deoxyribose, *J. Chem. Phys.*, 120(18), pp. 8505-8511.
47. Sanchez-Estrada, F. S., Qiu, H., and Timmons, R. B. **(2002)**. Molecular tailoring of surfaces via RF pulsed plasma polymerization: Biochemical and other applications, in *Proc. IEEE Intr. Conf. Plasma*, pp.254.
48. Šašić, O., Dupljanin, S., de Urquijo, J., and Petrović, Z. L. **(2013)**. Scattering cross sections for electrons in C₂H₂F₄ and its mixtures with Ar from measured transport coefficients, *J. Phys. D: Appl. Phys.*, 46(32), 325201 (7pp).
49. Stokes, P. W., Casey, M. J. E., Cocks, D. J., de Urquijo, J., García, G., Brungerand, M. J., and White, R. D. **(2020)**. Self-consistent electron–THF cross sections derived using data-driven swarm analysis with a neural network model, *Plasma Sources Sci. Technol.*, 29 (11), 105008 (10pp).
50. Swadia, M., Thakar, Y., Vinodkumar, M., and Limbachiya, C. **(2017)**. Theoretical electron impact total cross sections for tetrahydrofuran (C₄H₈O) *Eur. Phys. J. D*, 71(4), 85 (5pp).
51. Swadia, M., Bhavsar, R., Thakar, Y., Vinodkumar, M., and Limbachiya, C. **(2017a)**. Electron-driven processes for furan, tetrahydrofuran and 2, 5-dimethylfuran, *Mol. Phys.*, 115(20), pp. 2521–2527.

52. Thiemer, B., Andreesen, J. R. and Schraeder, T. (2003). Cloning and characterization of a gene cluster involved in tetrahydrofuran degradation in *Pseudonocardia* sp. strain K1, *Arch. Microbiol.*, 179(4), pp. 266-277.
53. White, R. D., Brunger, M. J., Garland, N. A., Robson, R. E., Ness, K. F., Garcia, G., de Urquijo, J., Dujko, S., Petrović, Zoran Lj. (2014). Electron swarm transport in THF and water mixtures, *Eur. Phys. J. D*, 64(5), pp. 125 (6pp).
54. White, R. D., Tattersall, W., Boyle, G., Robson, R.E., Dujko, S., Petrovic, Z.Lj., Bankovic, A., Brunger, M.J., Sullivan, J.P., Buckman, S.J., and Garcia, G. (2014a). Low-energy electron and positron transport in gases and soft-condensed systems of biological relevance. *Applied Radiation and Isotopes*, 83 (Part B). pp. 77-85.
55. White, R. D., Cocks, D., Boyle, G., Casey, M., N Garland, N., Konovalov, D., Philippa, B., Stokes, P., de Urquijo, J., González-Magaña, O., McEachran, R. P., Buckman, S. J., Brunger, M. J., Garcia, G., Dujko, S., and Petrovic, Z Lj. (2018). Electron transport in biomolecular gaseous and liquid systems: theory, experiment and self-consistent cross-sections, *Plasma Sources Sci. Technol.* 27(5), 053001 (15pp).
56. Wolff, W., Rudek, B., da Silva, L. A., Hilgers, G., Montenegro, E. C., and Homem, M. G. P. (2019). Absolute ionization and dissociation cross sections of tetrahydrofuran: Fragmentation-ion production mechanisms, *J. Chem. Phys.*, 151(6), 064304 (13pp).
57. Zecca, A., Perazzolli, C., and Brunger, M. J. (2005). Positron and electron scattering from tetrahydrofuran, *J. Phys. B: At.Mol. Opt. Phys.*, 38(13), pp. 2079–2086.
58. Zhang, L., Sun, W., Zhang, Y., Fan, Z., Hu, S. and Fan, Q. (2017). Predicting differential cross sections of electron scattering from tetrahydrofuran, **J. Phys. B: At. Mol. Opt. Phys.**, 50(8), 085201 (13pp).
59. Zubek, M., Dampc, M., Linert, I., and Neumann, T. (2011). Electronic states of tetrahydrofuran molecules studied by electron collisions, *J. Chem. Phys.*, 135(13), 134317 (7pp).
60. Ganesh Babu Loganathan, Praveen M., Jamuna Rani D., “Intelligent classification technique for breast cancer classification using digital image processing approach” *IEEE Xplore Digital Library* 2019, Pp.1-6.
61. M. Viswanathan, Ganesh Babu Loganathan, and S. Srinivasan, “IKP based biometric authentication using artificial neural network”, *AIP Conference Proceedings* (2020), Volume 2271, Issue 1, pp 030030.
62. Mohammed Abdulghani Taha and Ganesh Babu Loganathan, “Hybrid algorithms for spectral noise removal in hyper spectral images” *AIP Conference Proceedings* (2020), Volume 2271, Issue 1, pp 030013.
63. Dr.Idris Hadi Salih, Ganesh Babu Loganathan, ”Induction motor fault monitoring and fault classification using deep learning probabilistic neural network” *Solid State Technology*(2020), Volume 63, Issue 6, PP No. 2196-2213.
64. Ganesh Babu Loganathan “Design and analysis of high gain Re Boost-Luo converter for high power DC application”, *Materials Today: Proceedings*(2020), Volume 33, Part 1, PP 13-22.
65. Ganesh Babu Loganathan, Dr.E.Mohan, R.Siva Kumar, “ Iot Based Water And Soil Quality Monitoring System”, *International Journal of Mechanical Engineering and Technology (IJMET)*(2019), Vol.10 Issue No.2, P.No. 537-541.

66. Suganthi K, Idris Hadi Salih, Ganesh Babu Loganathan, and Sundararaman K, "A Single Switch Bipolar Triple Output Converter with Fuzzy Control", *International Journal of Advanced Science and Technology*, (2020), Vol. 29, No. 5, (2020), P.No.. 2386 – 2400.
67. Ganesh Babu Loganathan, "Can Based Automated Vehicle Security System", *International Journal of Mechanical Engineering and Technology (IJMET)*(2019), Vol.10 Issue No.07, P.No. 46-51.
68. B.K. Patle, Ganesh Babu L, Anish Pandey, D.R.K. Parhi, A. Jagadeesh, A review: On path planning strategies for navigation of mobile robot, *Defence Technology*, Volume 15, Issue 4, August 2019, Pages 582-606.
69. Dr.A.Senthil Kumar, Dr.Venmathi A R ,L.Ganesh Babu, Dr.G. Suresh, "Smart Agriculture Robo With Leaf Diseases Detection Using IOT", *European Journal of Molecular & Clinical Medicine*, Volume 07, Issue 09, PP 2462-2469.
70. Ganesh Babu L 2019 Influence of benzoyl chloride treatment on the tribological characteristics of Cyperus pangorei fibers based nonasbestos brake friction composites *Mater. Res. Express* 7 015303.
71. Manoharan S, Sai Krishnan G, Babu L G, Vijay R and Singaravelu D L 2019 Synergistic effect of red mud-iron sulfide particles on fade recovery characteristics of non-asbestos organic brake friction composites *Mater. Res. Express* 6 105311.
72. Manoharan S, Shihab A I, Alemdar A S A, Ganesh Babu L, Vijay R and Lenin Singaravelu D 2019 Influence of recycled basalt-aramid fibres integration on the mechanical and thermal properties of brake friction composites *Material Research Express* 6 115310.
73. G Sai Krishnan , L Ganesh Babu, P Kumaran , G Yoganjaneyulu and Jeganmohan Sudhan Raj, "Investigation of Caryota urens fibers on physical, chemical, mechanical and tribological properties for brake pad applications", *Material Research Express* 7 015310
74. A.Devaraju, P.Sivasamy, Ganesh Babu Loganathan, "Mechanical properties of polymer composites with ZnO nano-particle", *Materials Today: Proceedings*(2020), Volume 22, Part 3, Pages 531-534
75. Qaysar S.Mahdi, "Prediction of Mobile Radio Wave Propagation in Complex Topography", *Eurasian Journal of Science & Engineering*, Volume 4, Issue 1 (Special Issue); September, 2018, PP 49-55.
76. Qaysar S. Mahd, "Survivability Analysis of GSM Network Systems", *Eurasian Journal of Science & Engineering*, Volume 3, Issue 3; June, 2018, PP 113-123.
77. Qaysar S.Mahdi, "Comparison Study of Multi-Beams Radar under Different Radar Cross Section and Different Transmitting Frequency", *Eurasian Journal of Science & Engineering*, Volume 3, Issue 3; June, 2018, PP 1-11.
78. Qaysar Salih Mahdi, Idris Hadi Saleh, Ghani Hashim, Ganesh Babu Loganathan, "Evaluation of Robot Professor Technology in Teaching and Business", *Information Technology in Industry*, Volume 09, Issue 01, PP 1182-1194.
79. Ellappan Mohan, Arunachalam Rajesh , Gurram Sunitha , Reddy Madhavi Konduru , Janagaraj Avanija, Loganathan Ganesh Babu, "A deep neural network learning-based speckle noise removal technique for enhancing the quality of synthetic-aperture radar images", *Concurrency And Computation-Practice & Experience*, <https://doi.org/10.1002/cpe.6239>.

80. Dr.A.Senthil Kumar, Dr.G.Suresh, Dr.S.Lekashri, Mr.L.Ganesh Babu, Dr. R.Manikandan, "Smart Agriculture System With E – Carbage Using Iot", *International Journal of Modern Agriculture*, Volume 10, No.1, 2021 pp 928-931.
81. Ganesh Babu Loganathan, Idris Hadi Salih , A.Karthikayen, N. Satheesh Kumar, Udayakumar Durairaj. (2021). EERP: Intelligent Cluster based Energy Enhanced Routing Protocol Design over Wireless Sensor Network Environment. *International Journal of Modern Agriculture*, 10(2), 1725 - 1736. Retrieved from <http://www.modern-journals.com/index.php/ijma/article/view/908>
82. Dr.A.Senthil Kumar, Dr.G.Suresh, Dr.S.Lekashri, Mr.L.Ganesh Babu, Dr. R.Manikandan. (2021). Smart Agriculture System With E – Carbage Using Iot. *International Journal of Modern Agriculture*, 10(1), 928 - 931. Retrieved from <http://www.modern-journals.com/index.php/ijma/article/view/690>.
83. C. Kannan, Nalin Kant Mohanty, R. Selvarasu,"A new topology for cascaded H-bridge multilevel inverter with PI and Fuzzy control", *Energy Procedia*, Volume 117, 2017,Pages 917-926, ISSN 1876-6102, <https://doi.org/10.1016/j.egypro.2017.05.211>.
84. C. Kannan, and C.K. Kishore, "A Comparision of Three Phase 27 Level Inverter Scheme under No Load and Multiple Load Conditions", *Bulletin of Electrical Engineering and Informatics* Vol. 3, No.4, pp. 245-250, December 2014
85. S Priyadharsini, TS Sivakumaran, C Kannan, "Performance analysis of photovoltaic-based SL-quasi Z source inverter" *International Journal of Energy Technology and Policy*, Volume 1, Issue 3, Pages 254-264.
86. Maheswari, V. , Nandagopal, V. and Kannan, C. (2016), "Performance Metric of Z Source CHB Multilevel Inverter FED IM for Selective Harmonic Elimination and THD Reduction", *Circuits and Systems*, **7**, 3794-3806. doi: 10.4236/cs.2016.711317.
87. Nandagopal, Dr.V., Maheswari, Dr.V. and Kannan, C. (2016) Newly Constructed Real Time ECG Monitoring System Using LabView. *Circuits and Systems*, **7**, 4227-4235.
88. Mohammad Mustafa Othman, Sherzad Aziz Taha, and Jwan Jalal Mohammad, "Electron transport parameters in Hydrogen–argon mixtures", *AIP Conference Proceedings* (2017), Volume 1888, pp 020040.
89. Dr.Mohammad M. Othman , Dr.Idris H. Salih , Dr.Sherzad A.Taha, Electron Transport Properties In Tetramethylsilane Vapour, *Solid State Technology*(2020), Volume 63, Issue 6, PP No. 10188-10200.
90. M. Othman, M., taha, sherzad and Rasool Hussein, S. (2020) "Boltzmann equation studies on electron swarm parameters for oxygen plasma by using electron collision cross – sections", *Zanco Journal of Pure and Applied Sciences*, 32(5), pp. 36-53. doi: 10.21271/ZJPAS.32.5.4.
91. BABU LOGANATHAN, ganesh; E.MOHAN, Dr.. High Quality Intelligent Database Driven Microcontroller Based Heartbeat Monitoring System. *International Journal of Engineering & Technology*, [S.l.], v. 7, n. 4.6, p. 472-476, sep. 2018. ISSN 2227-524X.
92. Othman, M., Taha, S. and Salih, I. (2019) "Analysis of Electron Transport Coefficients in SiH4 Gas Using Boltzmann Equation in the Presence of Applied Electric Field", *Zanco Journal of Pure and Applied Sciences*, 31(1), pp. 77-88. doi: 10.21271/zjpas.31.1.10.